Vol. 316: 85–93, 2006 | MARINE ECOLOGY PROGRESS SERIES
Mar Ecol Prog Ser | Published July 3

Light absorption of *Isochrysis galbana* (Prymnesiophyceae) under a day–night cycle with ultraviolet radiation

Nobuaki Ohi[1,2,*], Akemi Mizobuchi[1], Satoru Taguchi[1]

[1]**Department of Environmental Engineering for Symbiosis, Soka University, 1-236 Tangi-cho, Hachiouji, Tokyo 192-8577, Japan**

[2]***Present address:*** **National Aeronautics and Space Administration, Hydrospheric and Biospheric Sciences Laboratory, Goddard Space Flight Center, Wallops Island, Virginia 23337, USA**

ABSTRACT: Diel variation in chlorophyll *a*-specific absorption coefficients, $a^*_{ph}(\lambda)$, m^2 (mg chl *a*)$^{-1}$, was examined to study the effect of ultraviolet radiation (UVR) on $a^*_{ph}(\lambda)$ of the prymnesiophycean *Isochrysis galbana* (Parke). A continuous culture was exposed for 2 wk to a 12 h light:12 h dark cycle of photosynthetically available radiation (PAR) supplemented with UVR. Photosynthetic and photoprotective pigments as well as cell density and diameter were also determined every 2 h for 2 d to confirm the periodicity of $a^*_{ph}(\lambda)$. A distinct diel variation was observed, with maxima toward the end of light periods and minima toward the end of dark periods. The magnitude of diel variation in $a^*_{ph}(440)$ and $a^*_{ph}(676)$ was 14 and 6.6%, respectively. To reconstruct the absorption coefficient, the absorption efficiency factors $Q_a(\lambda)$, were determined using intracellular chl *a* concentration, cell diameter, and chl *a*-specific absorption coefficients after solubilization on Triton X, $a^*_{TX}(\lambda)$. The main source of diel variation for $Q_a(\lambda)$ appears to be $a^*_{TX}(\lambda)$. Diel variation in the absorption ratio of photoprotective pigments to chl *a* was observed to be more significant than that for the absorption ratio of other photosynthetic pigments to chl *a*. The diel variations in $a^*_{ph}(\lambda)$ were primarily caused by changes in pigmentation of photoprotective pigments due to UVR.

KEY WORDS: Absorption · Diel cycle · Optical properties · Pigmentation · UV

INTRODUCTION

Studies on diel variations in optical properties have focused on the attenuation, scattering and absorption coefficients (Siegel et al. 1989, Dickey et al. 1990, Hamilton et al. 1990, Kroon et al. 1992, Stramska & Dickey 1992, Stramski & Reynolds 1993, Gardner et al. 1995, Stramski et al. 1995, DuRand & Olson 1996, 1998). Diel variations in the chlorophyll (chl) *a*-specific absorption coefficient, $a^*_{ph}(\lambda)$ (list of notations is provided in Table 1), have also sometimes been observed (Stramski & Reynolds 1993, Stramski et al. 1995). Ohi et al. (2002) showed recently that the coefficient of variation (CV) of diel variability in $a^*_{ph}(675)$ for the prymnesiophycean *Isochrysis galbana* was 9.3% under 500 µmol photons m^{-2} s^{-1} over a 12:12 h light–dark cycle. Diel variation in $a^*_{ph}(\lambda)$ can result from a combination of influences on pigmentation that are controlled by photoprotective and photosynthetic pigments (e.g. Sosik & Mitchell 1994) and pigment-packaging effects that vary with cell diameter and intracellular chl *a* concentration (e.g. Morel & Bricaud 1981). Distinct diel variations in $a^*_{ph}(\lambda)$ observed for *I. galbana* with maxima toward the end of dark periods and minima toward the end of light periods under 500 µmol photons m^{-2} s^{-1} were due to the package effect, but not the pigmentation (Ohi et al. 2002). However, diel variation in $a^*_{ph}(\lambda)$ has not been reported under illumination that includes UVR. Knowledge of the diel variation in $a^*_{ph}(\lambda)$ is important for determining the optical properties of phytoplankton and could contribute to interpretations of absorption properties

*Email: gtoi@hotmail.com

and estimates of primary productivity under illumination that includes UVR encountered in the surface layer of the ocean.

The efficiency factor for absorption, $Q_a(\lambda)$, is the ratio of the energy absorbed within a cell to the energy incident on its geometrical cross section. $Q_a(\lambda)$ and $a^*_{ph}(\lambda)$ can be reconstructed from the intracellular chl *a* concentration, cell diameter and the unpackaged chl *a*-specific absorption coefficients after solubilization in Triton X. Such reconstruction allows us to determine whether the observed absorption properties are fully consistent with reconstructed $a^*_{ph}(\lambda)$, and predictable from cell characteristics. This reconstruction is also aimed at determining the respective contributions of factors responsible for changes in the absorption properties of phytoplankton cells.

In the experiments reported here on diel variations in $a^*_{ph}(\lambda)$ of a phytoplankton species, we chose the prymnesiophycean *Isochrysis galbana* because similarly-sized nanoplankton cells are known to contribute significantly to the bulk optical properties of open-ocean waters (DuRand & Olson 1996). The aims of this study were therefore (1) to describe the diel variability in light-absorption properties of *I. galbana* at 500 µmol photons m^{-2} s^{-1} in the presence of UVR; (2) to differentiate between package effects and pigmentation effects on the diel variation in $a^*_{ph}(\lambda)$ under illumination that includes UVR; (3) to reconstruct the $a^*_{ph}(\lambda)$ spectra from the cell characteristics and to determine how the package effect and pigmentation effect contribute to the diel variations in $a^*_{ph}(\lambda)$ under the presence of UVR.

Table 1. Definition of mathematical symbols and associated units used in present paper. –: dimensionless

Symbol	Definition	Units
CV	Coefficient of variation throughout a diel cycle	%
λ	Wavelength	nm
OD (λ)	Optical density at a given wavelength	–
[chl *a*]	Chlorophyll *a* concentration	mg m^{-3}
$a_{ph}(\lambda)$	Absorption coefficient of phytoplankton	m^{-1}
$a_{TX}(\lambda)$	Absorption coefficient after solubilization in Triton X-100	m^{-1}
$a_{rec}(\lambda)$	Reconstructed absorption coefficient of phytoplankton	m^{-1}
$a_{total}(\lambda)$	Absorption coefficient of total pigments	m^{-1}
$a_{pig}(\lambda)$	Absorption coefficient of pigment *p*	m^{-1}
$a_{chl\ a}(\lambda)$	Absorption coefficient of chl *a*	m^{-1}
$a_{chl\ c}(\lambda)$	Absorption coefficient of chl c_{1+2}	m^{-1}
$a_{fuco}(\lambda)$	Absorption coefficient of fucoxanthin	m^{-1}
$a_{DD+DT}(\lambda)$	Absorption coefficient of diadinoxanthin plus diatoxanthin	m^{-1}
$a_{\beta,\beta\text{-carotene}}(\lambda)$	Absorption coefficient of β,β-carotene	m^{-1}
$a^*_{i,p}(\lambda)$	Weight-specific absorption coefficient of pigment *p*	m^2 (mg chl *a*)$^{-1}$
$a^*_{ph}(\lambda)$	Chlorophyll *a*-specific absorption coefficient	m^2 (mg chl *a*)$^{-1}$
$a^*_{TX}(\lambda)$	Chlorophyll *a*-specific absorption coefficient after solubilization in Triton X-100	m^2 (mg chl *a*)$^{-1}$
$a^*_{rec}(\lambda)$	Reconstructed chl *a*-specific absorption coefficient	m^2 (mg chl *a*)$^{-1}$
$a_{cm}(\lambda)$	Absorption coefficient of cell material	m^{-1}
N	Number of cells	cells
V	Volume of suspension	m^3
d	Mean cell diameter of population	µm
$Q_a(\lambda)$	Efficiency factor for absorption	–
$Q_a^*(\lambda)$	Package-effect index	–
ρ′	Optical thickness along the particle diameter	–
$c_{i,p}$	Intracellular concentration of pigment *p*	kg m^{-3}
$c_{chl\ a}$	Intracellular chl *a* concentration	kg m^{-3}

MATERIALS AND METHODS

Culture procedure and sampling. Culture conditions and experimental procedures have been described in detail by Ohi et al. (2002, 2003). Prymnesiophyceae *Isochrysis galbana* Parke (NEPCC 633) were obtained from The North East Pacific Culture Collection (NEPCC) at the University of British Columbia, Canada. *I. galbana* was grown on a 12 h light:12 h dark cycle at 25°C in a 1.4 l, quartz, culture vessel in seawater enriched with f/2 medium (Guillard & Ryther 1962). Careful axenic techniques were used to minimize bacterial contamination in the maintenance and growth of the culture. Visible radiation was from National cool-white fluorescent tubes (FL30S·EX-N) providing a quantum scalar irradiance of 500 µmol photons m^{-2} s^{-1} (photosynthetically available radiation, PAR, 400 to 700 nm) measured by a Biospherical Instrument QSL-100 4π sensor immersed in a water-filled culture vessel. Ultraviolet radiation (UVR), predominantly UV-B, was from Toshiba ultraviolet tubes (FL202·E) (see Fig. 2 in Taira et al. 2004) covered with acetate film (<290 nm cutoff, Polymer Plastics Corporation) (See Fig. 1 in Taira et al. 2004). The acetate film was changed every 5 d. The UVR dose-rate was measured by a Biospherical Instrument PUV-510 surface radiometer. The instrument provided UVR measurements at 308, 320, 340 and 380 nm. The photon-fluence density at 280 nm was assumed to be 0 mW m^{-2} nm^{-1}, since the FL202E UV lamp does not emit light <280 nm (see Fig. 2 in Taira et al. 2004). In order to

obtain absolute values of UVB, light intensities were integrated from 280 to 320 nm for the >280 nm treatment. UVA intensity was also integrated from 320 to 400 nm. Biologically effective irradiances for different treatments were determined as described by Smith & Baker (1979) and Smith et al. (1980) using the DNA weighting function of Stelow (1974), the generalized plant function of Caldwell (1971) and the chloroplast photoinhibition function of Jones & Kok (1966). Weightings and UV irradiances for intermediate wavelengths were calculated by linear interpolation.

The culture was operated in a continuous turbidostat with the dilution rate dictated by the growth rate of cells. The culture was acclimated to PAR for 11 d and PAR + UVR for 9 d. Cells were kept in suspension by a combination of continuous stirring and bubbling sterile air.

At each sampling, fresh media were added via a peristaltic pump to maintain relatively constant cell density (no./vol, N/V) within the optically thin suspension. The N/V averaged 4.3×10^{12} cells m^{-3} throughout the experiment. Separate duplicate sampling were initiated for the determination of absorption coefficient and pigments every 2 h for 48 h. These samples were filtered onto 25 mm GF/F glass-fiber filters (Whatman) under pressure lower than 100 mm Hg.

Cell number and diameter. Samples were preserved by adding 10% neutralized formaldehyde to obtain a 0.2% final concentration, and stored in the dark at 4°C. We confirmed that such treatment for this species induced only minor changes in cell diameter (<5%). Cell numbers were measured under a microscope with a hemacytometer (Bright-Line, Erma). Every 2 h, growth rate was calculated from the logarithm variations in cell abundance and dilution rate. Spherical cell diameters of 75 cells were measured under the microscope with an ocular ruler at 1000× magnification. The average cell volume was calculated from the average cell diameter, d, under the assumption that all cells were spherical.

Absorption coefficients. Optical densities, OD(λ), of suspensions were determined with a Shimadzu UV-2450 spectrophotometer equipped with an integrating sphere, with reference to a filtrate of the suspension (Whatman GF/F glass-fiber filter). OD (λ) was measured by placing the cuvettes at the entrance to an integrating sphere that minimized losses due to light-scattering. Absorption coefficients, $a_{ph}(\lambda)$, were obtained as follows (van de Hulst 1957):

$$a_{ph}(\lambda) = 2.3\ OD(\lambda)/r \quad (1)$$

where r (= 0.01 m) is the pathlength of the cuvette. Spectral values of the absorption coefficient were recorded every 1 nm from 350 to 750 nm. All spectra were set to zero at 750 nm to minimize differences between sample and reference, assuming lack of absorption by particles at 750 nm (Babin & Stramski 2002). The spectral absorption at all other wavelengths was also corrected for that offset at 750 nm. The chl *a*-specific absorption coefficients $a^*_{ph}(\lambda)$ were obtained from the absorption coefficients $a_{ph}(\lambda)$, according to:

$$a^*_{ph}(\lambda) = a_{ph}(\lambda)/[\text{chl } a] \quad (2)$$

where [chl *a*] is chlorophyll *a* concentration.

To differentiate between package and pigmentation effects on the diel variation in $a^*_{ph}(\lambda)$, cells were solubilized in the detergent Triton X-100 at a final concentration of 0.5% (in volume) with subsequent sonication as recommended by Berner et al. (1989). The Triton extracts were centrifuged, and spectral absorption $a_{TX}(\lambda)$ was determined on these solubilized cells with 0.5% Triton X-100 in filtered seawater as reference. These chl *a*-specific absorption coefficients for samples solubilized in Triton X-100, $a^*_{TX}(\lambda)$ were calculated as described for $a^*_{ph}(\lambda)$. Because the Triton X removes the effect of packaging pigments from the cells and chloroplasts, any changes in $a^*_{TX}(\lambda)$ are due only to changes in the pigmentation. The Triton X method involves spectral shifts in the wavelengths of peak absorption compared to *in vivo* absorption (Sosik & Mitchell 1991). In fact, we have observed shifts toward shorter wavelengths of 1 nm at the blue peak and 8 nm at the red peak. To compensate for these shifts, when using $a^*_{TX}(\lambda)$ in calculations or comparison with $a^*_{ph}(\lambda)$, we shifted the spectra by 1 nm for wavelengths of 350 to 557 nm and 8 nm for wavelengths of 551 to 750 nm. The region between 551 and 557 nm was repeated to prevent introduction of a gap in the spectra; values were relatively low and uniform at these wavelengths, so this treatment did not distort the spectra.

Pigments. The filtered samples were sonificated for 10 min in 10 ml of 90% acetone, and extracted for 24 h at 4°C. Following extraction, pigment samples were centrifuged for 5 min to remove cellular debris. Pigment analysis was carried out by HPLC (System Gold, Beckman) using the solvent gradient-system described by Head & Horne (1993). Identified pigments were chl c_{1+2}, fucoxanthin, diadinoxanthin, diatoxanthin, chl *a* and β,β-carotene. Integrated peak areas were quantified with external standards obtained from the 'International Agency for ^{14}C Determination', Denmark.

Reconstruction of absorption-efficiency factors from cell characteristics and package effect. Cells are assumed to be spherical and homogeneous with respect to the refractive index when the anomalous diffraction approximation is made (van de Hulst 1957). The reconstructed chl *a*-specific absorption coefficients $a^*_{rec}(\lambda)$ can be estimated by dividing the reconstructed absorption coefficients $a_{rec}(\lambda)$ by [chl *a*]. The $a_{rec}(\lambda)$ can be estimated using the number of cells, N, in a volume of the

suspension, V, the efficiency factors for absorption, $Q_a(\lambda)$ and the geometrical cross section determined by spherical cell diameter d (Morel & Bricaud 1981):

$$a_{rec}(\lambda) = N/V \cdot Q_a(\lambda) \cdot (\pi/4)\ d^2 \quad (3)$$

The $Q_a(\lambda)$ for a single cell, i.e. the ratio of absorbed to energy incident on the geometrical cross section of the cell, can be estimated (van de Hulst 1957) as:

$$Q_a(\lambda) = 1 + 2\exp[-\rho'(\lambda)] / \rho'(\lambda) + 2\{\exp[-\rho'(\lambda)] - 1\} / [\rho'(\lambda)^2] \quad (4)$$

where $\rho'(\lambda)$ is the dimensionless optical thickness of the particles. The $\rho'(\lambda)$ were here computed from $a^*_{TX}(\lambda)$ (Sosik & Mitchell 1991), intracellular chl a concentration, $c_{chl\ a}$, and d according to:

$$\rho'(\lambda) = a^*_{TX}(\lambda) \cdot c_{chl\ a} \cdot d \quad (5)$$

where $c_{chl\ a}$ is the ratio of [chl a] to the product of cell volume and cell density:

$$c_{chl\ a} = [\text{chl } a] / [(\pi/6)\ d^3 \cdot N/V] \quad (6)$$

The intracellular concentrations of various pigments p, $c_{i,p}$, were computed from each pigment, p, using Eq. (6). The fractional reduction of absorption due to the package effect $Q_a^*(\lambda)$ is computed (Morel & Bricaud 1981) as:

$$Q_a^*(\lambda) = (3/2) \cdot Q_a^*(\lambda)/\rho'(\lambda) \quad (7)$$

Contribution of pigmentation to $a^*_{ph}(\lambda)$. We examined pigmentation, which affected the magnitude of diel variation in $a^*_{ph}(440)$. The contribution of each pigment to the variation in $a^*_{ph}(\lambda)$ is equal to the product of the intracellular concentrations of various pigments, $c_{i,p}$, and the pigment-specific absorption coefficients. Absorption coefficients of various pigments, $a_{pig}(\lambda)$, were related to absorption coefficients of total pigments, $a_{total}(\lambda)$, according to:

$$a_{pig}(\lambda)/a_{total}(\lambda) = [c_{i,p} \cdot a^*_{i,p}(\lambda)] / [\sum_{i=1}^{n} c_{i,p} \cdot a^*_{i,p}(\lambda)] \quad (8)$$

where the value for the weight-specific absorption coefficient of pigment p, $a^*_{i,p}(\lambda)$, was the weight-specific absorption coefficient proposed by Fujiki & Taguchi (2001). This technique does not take into account pigment-packaging effects, but resolves issues regarding spectral shape and molar absorption coefficients. Despite these problems, the method allowed us to assess the relative importance of pigmentation to diel variation in $a^*_{ph}(\lambda)$.

Mathematical and statistical analysis. The periodicity of the rhythm was analyzed by a modified function of the cosine function (Halberg et al. 1978, Kieding et al. 1984) as:

$$Y = A + B\sin(t\pi/12) + C\cos(t\pi/12) \quad (9)$$

where Y is an estimate of a diel variable [e.g. $a^*_{ph}(\lambda)$, cell diameter, etc.], A is the average of the diel variable, t is time in hours. B is the amplitude of the sine function and C is the amplitude of the cosine function; thus, the amplitude of the rhythm is calculated as $(B^2 + C^2)^{1/2}$. A linear least-squares regression analysis was used to test the degree of fit of the estimated value to the observed value.

The magnitude of diel variation (%) for each variable was calculated as:

$$\text{Magnitude of diel variation} = |\max - \min| / \min \times 100 \quad (10)$$

where max is $A + (B^2+C^2)^{1/2}$ and min is $A - (B^2+C^2)^{1/2}$.

RESULTS

Biologically weighted UV irradiances (280 to 400 nm) for the biological weighting function tabulated by Smith et al. (1980) were 2.56 mW m^{-2} for DNA, 7.65 mW m^{-2} for plant and 46.78 mW m^{-2} for photoinhibition, respectively. Unweighted UVB (280 to 320 nm) and UV (280 to 400 nm) irradiances were 52.77 and 157.31 mW m^{-2}, respectively. UV irradiances for the acetate film filtered FL202·E UVR lamps weighting by the photoinhibition of photosynthesis function were over 18 times greater for PAR+UVR culture (46.78 mW m^{-2}, 290 to 400 nm) than when weighted by the DNA weighting function (2.56 mW m^{-2}, 290 to 400 nm). Unweighted irradiances of UVR and UVB were 157.31 mW m^{-2} at 290 to 400 nm and 52.76 mW m^{-2} at 290 to 320 nm, respectively, for the PAR + UVR culture. Additionally, the unweighted UVB irradiance (52.76 mW m^{-2})/PAR (500 µmol m^{-2} s^{-1}) ratio for the PAR + UVR culture was 0.1055. Total UVB exposures and the UVB/PAR ratio are similar or low for these experiments compared to daily average UVB irradiance (51.19 mW m^{-2}) and the UVB/PAR ratio (0.3385) at 10 m in the Florida Keys (see Table 1 in Lesser 2000). However, the UVB component was 33% of the total UVR irradiance, and was caused by the spectral shift of fluorescent tubes into the UVB portion of the spectrum. These unnatural radiation regimes were used here, as in other studies (e.g. Lesser et al. 2002), to examine the mechanistic effects on several processes related to the light absorption of photoinhibition for photosynthesis, and not spectral sensitivity as described above for the biological weighting-function calculations.

Mean growth rate calculated over a diel cycle (48 h) was 0.36 d^{-1} under PAR + UVR and 0.31 d^{-1} under 500 µmol m^{-2} s^{-1} PAR alone, respectively. Growth rates were not significantly different under PAR + UVR and PAR alone (Welch's t-test; $p > 0.05$).

The $a^*_{ph}(\lambda)$ spectra throughout a diel cycle exhibited absorption bands corresponding to chl a at around 440 and 676 nm, bands corresponding to accessory pig-

ments at around 460 and 490 nm, and spectral regions of relatively weak absorption between 586 and 635 nm (Fig. 1). The significant 1:1 linear relationship between all measured data in the present study (Table 2) and the data estimated by Eq. (9) indicate distinct diel variation. Distinct diel variations in measured $a^*_{ph}(\lambda)$ were observed for the red-absorption maximum at 676 nm and the blue-absorption maximum at 440 nm, with maxima toward the end of light periods and minima toward the end of dark periods ($p < 0.01$ at 440 and 676 nm) (Fig. 2). The magnitude of diel variation in $a^*_{ph}(\lambda)$ was 6.6% at 676 nm and 14% at 440 nm, respectively (Table 2).

In detergent-solubilized samples, the absorption peak shifted toward shorter wavelengths of 1 nm at the blue peak and 8 nm at the red peak. The spectral values of $a^*_{TX}(\lambda)$ are presented following adjustment (Fig. 1). Distinct diel variations in $a^*_{TX}(\lambda)$ were also present, with maxima toward the end of light periods and minima toward the end of dark periods ($p < 0.05$ at 676 and 440 nm) (Fig. 2). The magnitude of diel variation in $a^*_{TX}(\lambda)$ was 7.9% at 676 nm and 15% at 440 nm, respectively (Table 2).

A distinct diel variation was observed for [chl *a*], with maxima toward the end of dark periods and minima toward the end of light periods ($p < 0.001$). The magnitude of diel variation was −28% for [chl *a*] (minus sign of the magnitude of diel variation indicates decrease during the light periods) (Table 2). A distinct diel variation was not observed for N/V ($p > 0.05$). The coefficient of variation (CV) throughout a diel cycle was 9.9% for N/V; *d* exhibited a distinct diel variation, with maxima toward the end of light periods and minima toward the end of dark periods ($p < 0.001$) (Fig. 3). The magnitude of diel variation in *d* was 7.7% (Table 2). A distinct diel variation was obtained for $c_{chl\ a}$, with maxima toward the end of dark periods and minima toward the end of light periods ($p < 0.001$). The magnitude of diel variation in $c_{chl\ a}$ was −33% (minus sign of the magnitude of diel variation indicates decrease during the light periods).

The predominant pigments found in this study are in agreement with the previous findings of Zapata & Garrido (1997). Distinct diel variations were observed for the fucoxanthin/chl *a*, chl c_{1+2}/chl *a* and (diadinoxanthin plus diatoxanthin)/chl *a* ratios, with maxima

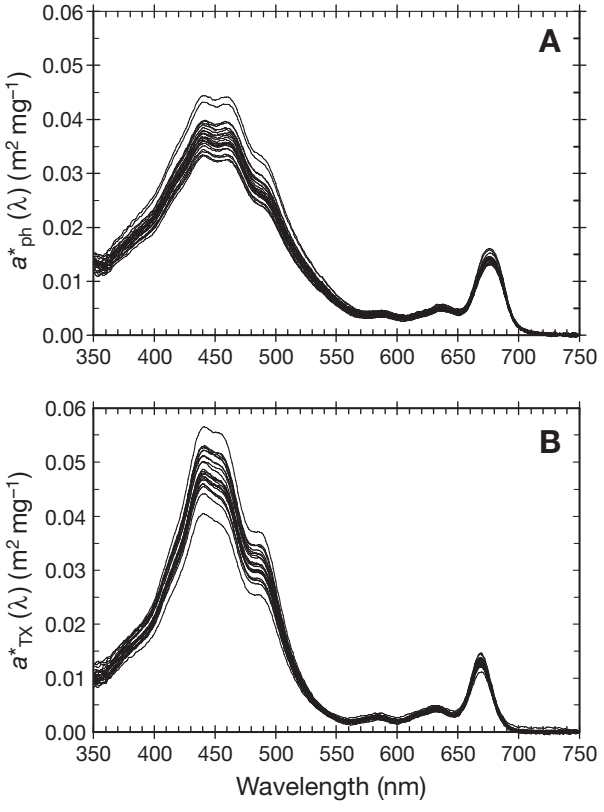

Fig. 1. *Isochrysis galbana*. Diel variations in spectral values of (A) chlorophyll *a*-specific absorption coefficients, $a^*_{ph}(\lambda)$, and (B) $a^*_{ph}(\lambda)$ after solubilization in 0.5% Triton X-100, $a^*_{TX}(\lambda)$. Each graph comprises 24 spectra determined throughout experiments

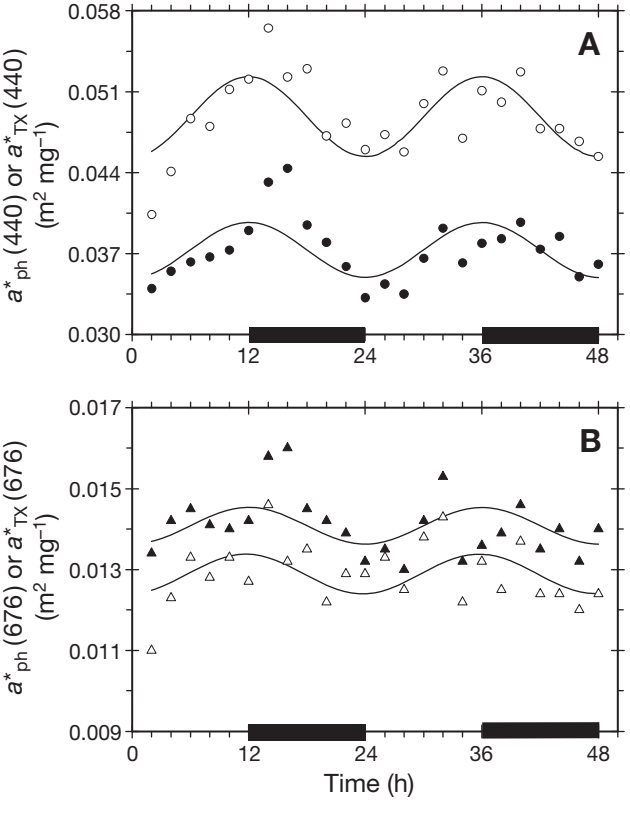

Fig. 2. *Isochrysis galbana*. Diel variations in chl *a*-specific absorption coefficients at (A) 440 nm, $a^*_{ph}(440)$ (●), or $a^*_{ph}(\lambda)$ after solubilization in 0.5% Triton X-100 at 440 nm, $a^*_{TX}(440)$ (○), and (B) $a^*_{ph}(676)$ (▲), or $a^*_{TX}(676)$ (△). Curve represents cosine fit to data; black bars indicate dark periods

Table 2. *Isochrysis galbana*. Chlorophyll *a* concentration [chl *a*], chl *a*-specific absorption coefficient (a^*_{ph} [λ]), a^*_{ph} (λ) after solubilization in 0.5% Triton X-100 (a^*_{TX} [λ]), reconstructed a^*_{ph} (λ) (a^*_{rec} [λ]), efficiency factor for absorption (Q_a [λ]) and computed package effect index (Q_a^* [λ]) at 440 and 676 nm, intracellular chl *a* concentration ($c_{chl\ a}$), mean cell diameter (d), pigment ratios (chl *c*:chl c_{1+2}; fuco: fucoxanthin; DD: diadinoxanthin; DT: diatoxanthin) and reconstructed absorption ratios of pigments to total pigment at 440 nm. Minimal and maximal values and magnitude of diel variation (%) of parameters estimated using cosine fit to data, as in Eq. (9) are shown. Minus signs indicate decrease during light periods; r^2 values are from linear regressions between all measured data and data estimated by Eq. (9)

Parameter	Max.	Min.	%	r^2
[chl *a*] (mg m^{-3})	686	534	−28.4	0.83
a^*_{ph} (440) (m^2 mg^{-1})	0.0397	0.0350	13.6	0.40
a^*_{ph} (676) (m^2 mg^{-1})	0.0145	0.0136	6.6	0.17
a^*_{TX} (440) (m^2 mg^{-1})	0.0523	0.0454	15.2	0.51
a^*_{TX} (676) (m^2 mg^{-1})	0.0134	0.0124	7.9	0.20
a^*_{rec} (440) (m^2 mg^{-1})	0.0414	0.0373	10.8	0.34
a^*_{rec} (676) (m^2 mg^{-1})	0.0126	0.0117	7.2	0.19
Q_a (440)	0.36	0.29	22.0	0.56
Q_a (676)	0.11	0.088	28.1	0.52
Q_a^* (440)	0.82	0.79	−3.9	0.32
Q_a^* (676)	0.95	0.93	−1.5	0.51
$c_{chl\ a}$ d (kg m^{-2})	13.8	11.0	−26.1	0.17
$c_{chl\ a}$ (kg m^{-3})	3.1	2.3	−32.5	0.17
d ($\times 10^{-6}$ m)	4.8	4.5	7.7	0.75
chl *c*/chl *a*	0.24	0.22	9.3	0.32
Fuco/chl *a*	0.43	0.39	10.4	0.42
DD+DT/chl *a*	0.25	0.20	24.1	0.46
$a_{chl\ a}/a_{total}$	0.49	0.45	−7.5	0.61
$a_{chl\ c}/a_{total}$	0.20	0.19	6.0	0.36
a_{DD+DT}/a_{total}	0.18	0.15	16.1	0.39

toward the end of light periods and minima toward the end of dark periods ($p < 0.05$) (Fig. 3). The increase in a^* (440) or a^*_{TX} (440) during the light periods (Fig. 2) was parallel to an increase in the fucoxanthin/chl *a* ratio by 10%, the chl c_{1+2}/chl *a* ratio by 9.3%, and the (diadinoxanthin plus diatoxanthin)/chl *a* ratio by 24% (Table 2). A distinct diel variation was not observed for β,β-carotene/chl *a* ($p > 0.05$). The coefficient of variation throughout a diel cycle was 7.5% for β,β-carotene/chl *a*.

The relative ratio in reconstructed absorption of each pigment to total pigment was examined. The reconstructed absorption of chl *a*, $a_{chl\ a}$(440), to the reconstructed absorption of total pigment, a_{total}(440), was from 45 to 49% throughout a diel cycle. The relative ratio of the various pigments to a_{total}(440) was followed by fucoxanthin, diadinoxanthin plus diatoxanthin, chl c_{1+2} and β,β-carotene, in that order. Distinct diel variations were observed for the ratios of a_{chlc} or a_{DD+DT} to a_{total} at 440 nm, with maxima toward the end of light periods and minima toward the end of dark periods ($p < 0.001$) (Fig. 4). In contrast, a distinct diel variation was observed for the ratios of $a_{chl\ a}$ to a_{total} at 440 nm, with a 12 h shift in the periodicity ($p < 0.001$) (Fig. 4). The increase in a^*_{ph}(440) during the light periods was parallel to the increase in the a_{chlc}/a_{total} ratio by 6.0% and the a_{DD+DT}/a_{total} ratio at 440 nm by 16%, with decreases in the $a_{chl\ a}/a_{total}$ ratio at 440 nm by 7.5% (Table 2). Distinct diel variations were not obtained for a_{fuco} and $a_{β,β\text{-carotene}}$ to a_{total} at 440 nm ($p > 0.05$). The coefficient of variation throughout a diel cycle was 3.1% for a_{fuco} to a_{total} at 440 nm and 5.9% for $a_{β,β\text{-carotene}}$ to a_{total} at 440 nm.

DISCUSSION

Shift in phase of diel cycle of a^*_{ph}(λ)

The diel pattern in a^*_{ph}(λ) under illumination that includes UVR was characterized by maxima toward the end of light periods and minima toward the start of light periods. However, an opposite diel pattern in a^*_{ph}(λ) for the same species *Isochrysis galbana* with maxima toward the end of dark periods and minima toward the end of light periods was observed under illumination comprised of PAR alone (500 µmol photons m^{-2} s^{-1}) (Ohi et al. 2002), compared to that under illumination that included UVR (Fig. 5). These diel variation in a^*_{ph}(440) (−22%) was primarily caused by changes in cell size (21%) due to a packaging effect under PAR alone. The present and previous results (Ohi et al. 2002) provide strong evidence that the same species of phytoplankton exhibits 12 h shifts in diel patterns of a^*_{ph}(λ) depending on UVR. The diel pattern of a^*_{ph}(λ) under illumination that included UVR indicated a 6 h shift compared to the pattern of 1500 µmol photons m^{-2} s^{-1} PAR alone (Ohi et al. 2003) (Fig. 5). The diel variation in a^*_{ph}(440) (50%) was primarily caused by changes in pigmentation of photoprotective pigments under high irradiance.

Reconstructed absorption coefficients and efficiency factors for absorption

Distinct diel variations in reconstructed a^*_{rec}(λ) were also observed, with maxima toward the end of light periods and minima toward the end of dark periods ($p < 0.01$ at 440 nm and $p < 0.05$ at 676 nm) (Fig. 6). The relationship between diel variation in experimental a^*_{ph}(440) and diel variation in reconstructed a^*_{rec}(440) was significantly correlated ($p < 0.001$); the slope of the

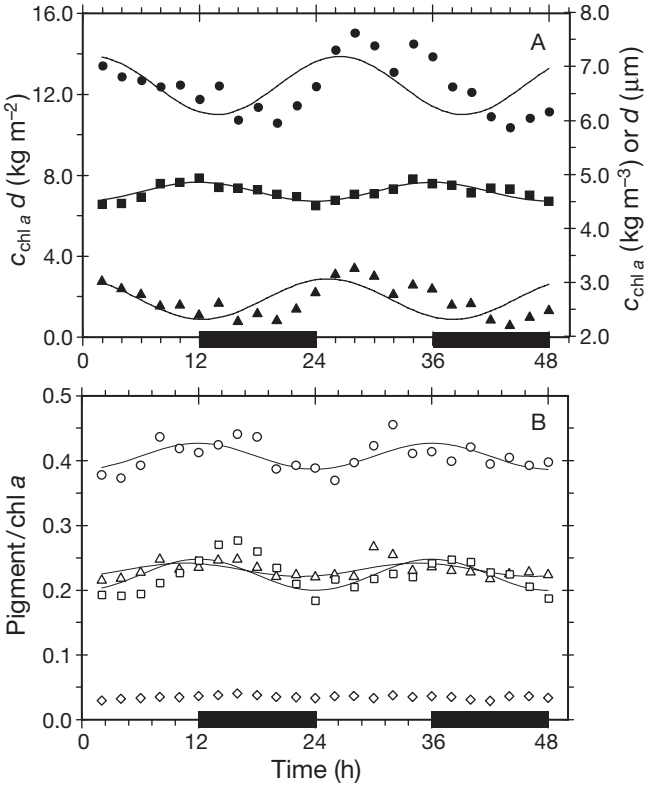

Fig. 3. *Isochrysis galbana*. Diel variations in (A) product of intracellular chlorophyll *a* concentration ($c_{chl\,a}$) and cell diameter (d) and ($c_{chl\,a}$) or d, and (B) ratios of pigments to chl *a*. (●) $c_{chl\,a}$ d; (▲) $c_{chl\,a}$; (■) d; (○) fucoxanthin; (□) diadinoxanthin plus diatoxanthin; (△) chl c_{1+2} (◇) and β,β-carotene. Curve represents cosine fit to data except for fucoxanthin and β,β-carotene; black bars indicate dark periods

regression line was 0.95. The reconstructed values were lower than the measured values by an average of 5%, although the reconstruction was fairly satisfactory. Therefore, this allows us to examine how the various parameters contributed to $a^*_{ph}(\lambda)$ variations over their diel cycle.

Distinct diel variations were observed for $Q_a(\lambda)$, with maxima toward the end of light periods and minima toward the end of dark periods ($p < 0.01$ at 440 and 676 nm) (Fig. 7). $Q_a(\lambda)$ ranged from 0.29 to 0.36 at 440 nm, and from 0.11 to 0.088 at 676 nm. For the range of $Q_a(\lambda)$ estimated, the $Q_a(\lambda)$ versus $\rho'(\lambda)$ relationship (Eq. 4) was linear (see Fig. 1 in Morel & Bricaud 1981). A quantitative evaluation of this effect can be made by computing the package-effect index $Q_a^*(\lambda)$. $Q_a^*(\lambda)$, which ranged from 1 (no package effect) to 0 (maximal package effect), was obtained using Eq. (7). Distinct, but gentle diel variations in $Q_a^*(\lambda)$ were observed, with maxima toward the end of dark periods and minima toward the end of light periods ($p < 0.01$ at 440 nm and $p < 0.001$ at 676 nm) (data not shown). $Q_a^*(\lambda)$ was remarkably constant at −3.9% for 440 nm and −1.5%

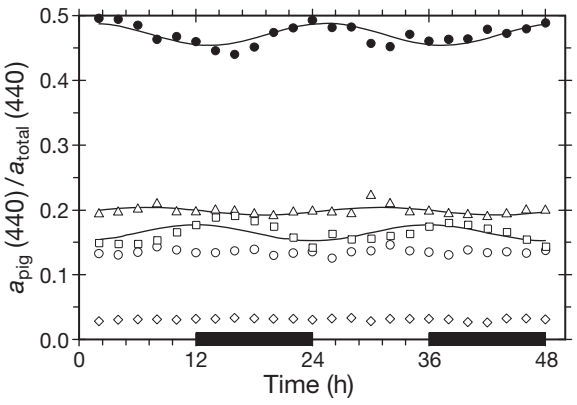

Fig. 4. *Isochrysis galbana*. Diel variations in reconstructed absorption ratios of pigments to total pigments, $a_{pig}(440)/a_{total}(440)$. (●) chl *a*; (○) fucoxanthin; (□) diadinoxanthin plus diatoxanthin; (△) chl c_{1+2}; (◇) β,β-carotene. Curve represents cosine fit to data except for fucoxanthin and β,β-carotene; black bars indicate dark periods

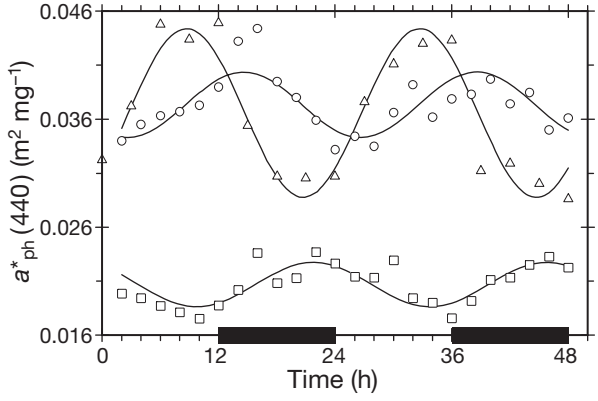

Fig. 5. *Isochrysis galbana*. Diel variations in chl *a*-specific absorption coefficients at 440 nm, $a^*_{ph}(440)$, under (○) 500 µmol m^{-2} s^{-1} PAR that included UVR (present study), (□) 500 µmol m^{-2} s^{-1} of PAR alone (Ohi et al. 2002), and (△) 1500 µmol m^{-2} s^{-1} PAR alone (Ohi et al. 2003). Curve represents cosine fit to data; black bars indicate dark periods

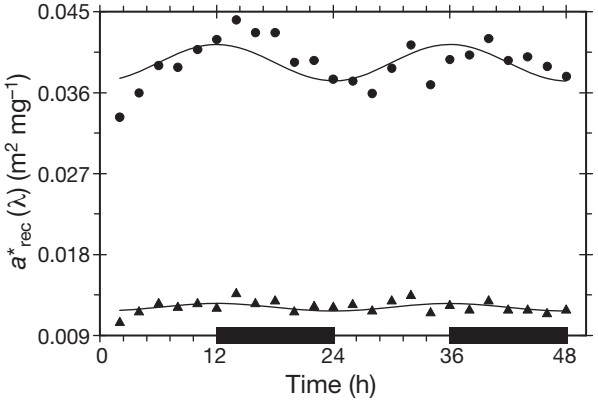

Fig. 6. *Isochrysis galbana*. Diel variations in reconstructed chl *a*-specific absorption coefficients $a^*_{rec}(\lambda)$, at (●) 440 and (▲) 676 nm. Curve represents cosine fit to data; black bars indicate dark periods

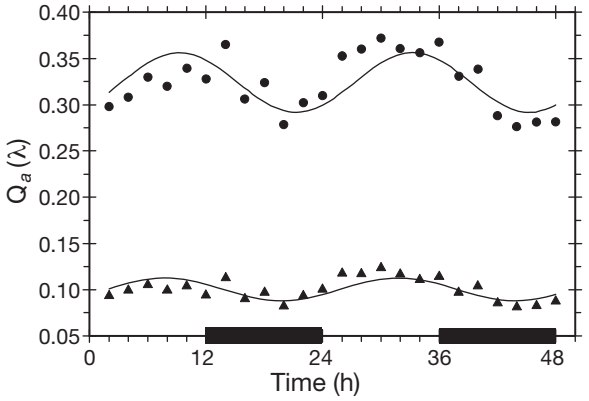

Fig. 7. *Isochrysis galbana*. Diel variations in reconstructed values of efficiency factor, $Q_a(\lambda)$, at (●) 440 and (▲) 676 nm. Curve represents cosine fit to data; black bars indicate dark periods

for 676 nm (Table 2). These variations in $Q_a^*(\lambda)$ indicated negligible package effects.

$Q_a(\lambda)$ was estimated from the product of the intracellular chl *a* concentration $c_{\text{chl }a}$, cell diameter *d*, and $a^*_{\text{TX}}(\lambda)$ (Eqs. 4 to 6). A distinct diel variation was observed for $a^*_{\text{TX}}(\lambda)$, with maxima toward the end of light periods and minima toward the end of dark periods, possibly due to photoacclimation ($p < 0.01$ at 440 nm and $p < 0.05$ at 676 nm) (Fig. 2). Distinct diel variations were obtained for $c_{\text{chl }a}\,d$, with a 12 h shift in periodicity ($p < 0.05$) (Fig. 3). Thus, a distinct diel variation was observed for $c_{\text{chl }a}\,d$, with maxima toward the end of dark periods and minima toward the end of light periods. However, a distinct but gentle diel variation was observed for *d*, with maxima toward the end of light periods and minima toward the end of dark periods ($p < 0.05$) (Fig. 3). Therefore, the main source of diel variation for $Q_a(\lambda)$ appears to be $a^*_{\text{TX}}(\lambda)$, which increased by 15% at 440 nm and 7.9% at 676 nm during the light periods (Fig. 2). $c_{\text{chl }a}\,d$, which decreased by 26% during the light periods (Fig. 3), reduced the diel variation in $Q_a(\lambda)$ by dampening the effect of $c_{\text{chl }a}\,d$ on $Q_a(\lambda)$. Any changes in $a^*_{\text{TX}}(\lambda)$ could have been due only to changes in the pigmentation, as described above.

Contribution of pigmentation to diel variation in $a^*_{\text{ph}}(\lambda)$

We examined the contribution of pigmentation and its effect on the diel variation in $a^*_{\text{ph}}(440)$. An increase in pigmentation due to changes in the relative proportions of chl *a* and accessory pigments during the light periods resulted from an increase in photoprotective pigments, especially the diadinoxanthin plus diatoxanthin to chl *a* ratio (Fig. 3). Similar results under a light:dark cycle at high-light irradiance have been observed for the photosynthetic and photoprotective pigment to chl *a* ratio (e.g. Kohata & Watanabe 1989) and diadinoxanthin plus diatoxanthin to chl *a* ratio (e.g. Demers et al. 1991). The increase in $a^*_{\text{ph}}(440)$ during the light periods was due mainly to both an increase in $a_{\text{DD+DT}}(440)$ and a decrease in $a_{\text{chl }a}(440)$ during the light periods over the diel cycle. The increase in $a^*_{\text{ph}}(440)$ during the light periods seemed to directly affect the amount of light energy absorbed.

Implication for field observations

The results of this study provide strong evidence that the $a^*_{\text{ph}}(\lambda)$ can increase during the day under a diel cycle in the surface layer of the ocean exposed to UVR. Diel patterns in photosynthetic and photoprotective pigments due to photoadaptation were the primary cause of the diel pattern in $a^*_{\text{ph}}(\lambda)$ under exposure to UVR. Since the diel patterns in pigmentation of *Isochrysis galbana* are similar to those of other phytoplankton species exposed to UVR, these results could be important for interpreting diel variations in optical properties of the ocean's surface-layer. The results presented here and published previously (Ohi et al. 2002) suggest that phytoplankton can exhibit 12 h shifts in diel patterns of $a^*_{\text{ph}}(\lambda)$ in the surface water-layer exposed to UVR. The measurement of light-depth dependent optical properties presents a new challenge for assessing the impact of this phenomenon on the procedures used for estimating phytoplankton biomass and production.

Acknowledgement. The manuscript was greatly improved by the comments of anonymous reviewers.

LITERATURE CITED

Babin M, Stramski D (2002) Light absorption by aquatic particles in the near-infrared spectral region. Limnol Oceanogr 47:911–915

Berner T, Dubinsky Z, Wyman K, Falkowski PG (1989) Photoadaptation and the 'package' effect in *Dunaliella tertiolecta* (Chlorophyceae). J Phycol 25:70–78

Caldwell MM (1971) Solar ultraviolet radiation and the growth and development of higher plants. In: Giese AC (ed) Photophysiology. Academic Press, New York, p 131–177

Demers S, Roy S, Gagnon R, Vignault C (1991) Rapid light-induced changes in cell fluorescence and in xanthophyll-cycle pigments of *Alexandrium excavatum* (Dinophyceae) and *Thalassiosira pseudonana* (Bacillariophyceae): a photo-protection mechanism. Mar Ecol Prog Ser 76: 185–193

Dickey T, Granata T, Hamilton M, Wiggert J, Marra J, Langdon C, Siegel DA (1990) Time series observations of bio-

optical properties in the upper layer of the Sargasso Sea. Proc Int Soc Opt Eng Ocean Optics 10:202–213
DuRand MD, Olson RJ (1996) Contributions of phytoplankton light scattering and cell concentration changes to diel variations in beam attenuation in the equatorial Pacific from flow cytometric measurements of pico-, ultra- and nanoplankton. Deep-Sea Res II 43:891–906
DuRand MD, Olson RJ (1998) Diel patterns in optical properties of the chlorophyte *Nannochloris* sp.: relating individual-cell to bulk measurements. Limnol Oceanogr 43: 1107–1118
Fujiki T, Taguchi S (2001) Relationship between light absorption and the xanthophyll-cycle pigments in marine diatoms. Plankton Biol Ecol 48:96–103
Gardner WD, Chung SP, Richardson MJ, Walsh ID (1995) The oceanic mixed-layer pump. Deep-Sea Res 42:757–775
Guillard RRL, Ryther JH (1962) Studies of marine planktonic diatoms. I. *Cyclotella nana* Hustedt and *Detonula confervacea* (Cleve) Gran. Can J Microbiol 8:229–239
Halberg F, Haus E, Scheving LE (1978) Sampling of biologic rhythms, chronocytokinetics and experimental oncology. In: Valleron AJ, Macdonald PDM (eds) Biomathematics and cell kinetics. Elsevier Biomedical Press, New York, p 175–190
Hamilton M, Granata TC, Dickey TD, Wiggert JD, Siegel DA, Marra J, Langdon C (1990) Diel variations of bio-optical properties in the Sargasso Sea. Proc Int Soc Opt Eng Ocean Optics 10 (1302):214–224
Head EJH, Horne PW (1993) Pigment transformation and vertical flux in an area of convergence in the North Atlantic. Deep-Sea Res II 40:329–346
Jones LW, Kok B (1966) Photoinhibition of chloroplast reactions. I. Kinetics and action spectra. Plant Physiol 41:1037–1043
Kieding N, Rudolph N, M?ller U (1984) Diurnal variation in influx and transition intensities in the S phase of hamster cheek pouch epithelium cells. In: Edmunds L Jr (ed) Cell cycle clocks. Marcel Dekker, New York, p 135–159
Kohata K, Watanabe M (1989) Diel changes in the composition of photosynthetic pigments and cellular carbon and nitrogen in *Pyramimonas parkeae* (Prasinophyceae). J Phycol 25:377–385
Kroon BMA, Latasa M, Ibelings BW, Mur LR (1992) The effect of dynamic light regimes on *Chlorella*. I. Pigments and cross sections. Hydrobiologia 238:71–78
Lesser MP (2000) Depth-dependent photoacclimatization to solar ultraviolet radiation in the Caribbean coral *Montastraea faveolata*. Mar Ecol Prog Ser 192:137–151
Lesser MP, Barry TM, Banaszak AT (2002) Effects of UV radiation on a chlorophyte alga (*Scenedesmus* sp.) isolated from the fumarole fields of Mt. Erebus, Antarctica. J Phycol 38:473–481
Morel A, Bricaud A (1981) Theoretical results concerning light absorption in a discrete medium, and application to specific absorption of phytoplankton. Deep-Sea Res 28: 1375–1393
Ohi N, Ishiwata Y, Taguchi S (2002) Diel patterns in light absorption and absorption efficiency factors of *Isochrysis galbana* (Prymnesiophyceae). J Phycol 38:730–737
Ohi N, Shino M, Ishiwata Y, Taguchi S (2003) Light absorption of *Isochrysis galbana* (Prymnesiophyceae) under day–night cycle at high-light irradiance. Plankton Biol Ecol 50:1–9
Siegel DA, Dickey TD, Washburn L, Hamilton MK, Mitchell BG (1989) Optical determination of particulate abundance and production variations in the oligotrophic ocean. Deep-Sea Res 36:211–222
Smith RC, Baker KS (1979) Penetration of UV-B and biologically effective dose-rates in natural waters. Photochem Photobiol 29:311–323
Smith RC, Baker KS, Holm-Hansen O, Olson RS (1980) Photoinhibition of photosynthesis in natural waters. Photochem Photobiol 31:585–592
Sosik HM, Mitchell BG (1991) Absorption, fluorescence, and quantum yield for growth in nitrogen-limited *Dunaliella tertiolecta*. Limnol Oceanogr 36:910–921
Sosik HM, Mitchell BG (1994) The effects of temperature on growth, light absorption and quantum yield in *Dunaliella tertiolecta* (Chlorophyceae). J Phycol 30:833–840
Stelow RB (1974) The wavelength in sunlight effective in producing skin cancer: a theoritical analysis. Proc Natl Acad Sci USA 71:157–191
Stramska M, Dickey TD (1992) Variability of bio-optical properties of the upper ocean associated with diel cycles in phytoplankton populations. J Geophys Res 97:17873–17887
Stramski D, Reynolds RA (1993) Diel variations in the optical properties of a marine diatom. Limnol Oceanogr 38: 1347–1364
Stramski D, Shalapyorok A, Reynolds RA (1995) Optical characterization of the oceanic unicellular cyanobacterium *Synechococcus* grown under a day–night cycle in natural irradiance. J Geophys Res 100:13295–13307
Taira H, Goes JI, Gomes HR, Yabe K (2004) Photoinduction of mycosporine-like amino acids and cell volume increases by ultraviolet radiation in the marine dinoflagellate *Scrippsiella sweeneyae*. Plankton Biol Ecol 51: 82–94.
van de Hulst HC (1957) Light scattering by small particles. Wiley-Liss, New York
Zapata M, Garrido JL (1997) Occurrence of phytylated chlorophyll *c* in *Isochrysis galbana* and *Isochrysis* sp. (clone T-ISO) (Prymnesiophyceae). J Phycol 33:209–214

Editorial responsibility: Otto Kinne (Editor-in-Chief), Oldendorf/Luhe, Germany

Submitted: April 19, 2005; Accepted: December 8, 2005
Proofs received from author(s): June 20, 2006